HYDROLOGICAL PROCESSES
Hydrol. Process. **23**, 1660–1667 (2009)
Published online 1 April 2009 in Wiley InterScience
(www.interscience.wiley.com) DOI: 10.1002/hyp.7311

Experimental study of extreme shear stress for shallow flow under simulated rainfall

Jau-Yau Lu,[1]* Jun-Ji Lee,[1] Tai-Fang Lu[2] and Jian-Hao Hong[1]

[1] *Department of Civil Engineering, National Chung Hsing University, Taichung, Taiwan, R.O.C.*
[2] *Department of Statistics and Informatics Science, Providence University, Taichung, Taiwan, R.O.C.*

Abstract:

The raindrop impact and overland flow are two major factors causing soil detachment and particle transportation. In this study, the turbulent characteristics of the shallow rain-impacted water flow were investigated using a 2-D fibre-optic laser Doppler velocimetry (FLDV) and an artificial rainfall simulator. The fluctuating turbulent shear stress was computed using digital data processing techniques. The experimental data showed that the Reynolds shear stress follows a probability distribution with heavy tails. The tail probability increases with an increase of rainfall intensity or raindrop diameter, and it decreases with an increase of Reynolds number. A modified empirical equation was derived using both the raindrop diameter and rainfall intensity as independent variables to provide a better prediction of the Darcy-Weisbach friction coefficient f under rainfall conditions. Copyright © 2009 John Wiley & Sons, Ltd.

KEY WORDS raindrop impact; turbulent shear stress; Darcy-Weisbach friction coefficient

Received 19 March 2008; Accepted 9 February 2009

INTRODUCTION

Soil erosion by water is the detachment and transportation of soil particles through the action of the runoff and raindrop splash over the soil surface. The extremely complex processes of detachment, transportation, and deposition are due to the spatial and temporal variations (Lu *et al*., 1987). The understanding of the mechanics of shallow flow with raindrop impact must be improved to properly predict and control the soil erosion.

Both experimental and numerical approaches have been used to investigate the turbulent properties of the shallow flows under simulated rainfall. Among others, Yoon and Wenzel (1971), Kisisel (1971), and Shahabian and Delleur (1976) used hot-film anemometer to perform their experimental studies. On the other hand, based on Chang (1996) and Liu's (1995) laboratory experiments conducted with a 2-D fibre-optic laser Doppler velocimetry (FLDV), Lu *et al*. (1998, 2001) investigated the characteristics of shallow rain-impacted flows over both smooth and rough beds, and proposed empirical formulas for the distributions of both the longitudinal and vertical turbulence intensities and the standard deviation of Reynolds stress. Wenzel and Wang (1970) investigated the mechanics of a single drop after striking a stagnant water layer based on both the numerical and experimental approaches. Hartley and Alonso (1991), as well as Hartley and Julien (1992) used the Volume of Fluid (VOF) method to calculate the spatial and temporal variations of boundary shear stress of a shallow water flow caused by a raindrop. Wu and Jiang (2007) incorporated a Gram-Charlier-type joint probability distribution of near-bed two-dimensional instantaneous velocity into a simple mechanistic model to study the turbulent bursting in sediment entrainment. In regard to the turbulent statistical characteristics, several experimental studies have been reported by Willmarth and Lu (1972), Lu and Willmarth (1973), Raupachu (1981), Kim *et al*. (1987), Balachandar and Bhuiyan (2007), and others.

Shen and Li (1973) found that for a flow Reynolds number less than 900, the Darcy-Weisbach friction factor increased with an increase of the rainfall intensity and a decrease of the flow Reynolds number. In general, for a two-dimensional steady uniform open-channel turbulent flow without rainfall, the mean total shear stress, which equals the sum of the viscous shear stress and turbulent (Reynolds) shear stress, varies linearly from a maximum value at the bed to zero at the free surface (Nezu and Nakagawa, 1993). Despite numerous investigations on the open channel flows, detailed measurements and statistical analyses of the flow characteristics of the raindrop-impacted shallow flows remain scarce. An interesting feature of the shallow flow under raindrop impact is that the applied shear stress is chaotic, which has important effect on the soil particle movement. Based on the laboratory data, Lu *et al*. (1998) found that the standard deviation of the Reynolds shear stress increases with rainfall intensity and raindrop diameter.

Wu (2006) conducted laboratory experiments to further increase the slope gradient to 1% for the shallow flows with raindrop impact. However, both Chang (1996) and Wu (2006) only analyzed the mean boundary shear stress in their study. The main objective of the present study

* Correspondence to: Jau-Yau Lu, Department of Civil Engineering, National Chung Hsing University, Taichung, Taiwan 402, R.O.C.
E-mail: jylu@mail.nchu.edu.tw

is to re-analyze the data collected by Chang (1996) and Wu (2006) in order to investigate the probability distributions of the near-bed turbulent shear stress and further increase our understanding of the shallow rain-impacted flows. Emphasis was placed on the detailed analysis of the extreme boundary shear stress.

METHOD

Experimental apparatus and procedure

Figure 1 shows a schematic layout of the flume and the artificial rainfall simulator adopted in this study. The rectangular recirculating flume was 12 m long, 0·5 m wide, 0·5 m high, and could be tilted up to 10%. The bed and side walls of the flume were 10-mm thick smooth glass plates. In order to exclude the suspended impurities, filters were placed in the settling tank. Furthermore, honeycombs and mesh screens were set up at the entrance of the channel to prevent the occurrence of large-scale disturbances and to achieve uniform inflow.

The velocity measurements were carried out with a two-component FLDV system with a 5-W argon-ion laser. The FLDV probe was moved by a three-dimensional traversing system that could be controlled with an accuracy of 0·001 mm. In this study, the 'even time mode' was selected. The time increment was 0·01 s (sampling frequency of 100 Hz), which was sufficiently small for water flow measurements.

A specially designed needle-type artificial rainfall simulator (1 m × 4 m) was used to generate rainfall with different raindrop sizes. A point gauge was also designed and used to measure the average water-surface elevation of the rain-impacted flow. More detailed descriptions of the features of the measuring equipment are given by Lu *et al*. (1998). The velocity measurements were performed at a section 8·6 m downstream from the channel entrance, which was near the midpoint of the rainfall region, with a fully developed flow.

The experimental treatments included four rainfall intensities, i.e. $I = 0.0, 50{\cdot}8, 76{\cdot}2$, and $101{\cdot}6$ mm/h (or 0, 2, 3, and 4 in/h), two drop sizes, i.e., $d = 3$ and 4 mm, and four slope gradients, i.e., $S = 0{\cdot}1\%, 0{\cdot}3\%, 0{\cdot}5\%$, and 1%. Two extreme cases under the conditions with and without rainfall are given in Table I. For the case with rainfall, the flow discharge (Q) at the measuring cross section (i.e., X = 8·6 m) was kept the same as that for the corresponding run without rainfall.

RESULTS

Mean velocity

Figures 2a and 2b give comparisons of the measured mean velocity profiles with and without rainfall under low and high Reynolds numbers, respectively. As shown in either figure, there is a very significant flow retardation near the water surface for the case with rainfall (R4 or R5) due to the raindrop impact. In Figure 2a, for case R4 the whole flow depth was completely penetrated by the raindrops, and the velocity profile near the channel boundary was more uniform than that for case NR1 because of the increased vertical mixing of the flow. On the other hand, in Figure 2b the velocity profiles near the channel boundary are very close for both curves, indicating that the raindrop effect is negligibly small near the channel bottom for the cases with high Reynolds numbers. The ratios between mean flow depth and raindrop diameter $\overline{H}/d$ are 1·92 and 2·84 for cases R1 and R5, respectively as shown in Table I.

Figures 3 and 4 show the normalized probability density functions of both longitudinal and vertical velocity components (u and v) at a position with $Y^+ \cong 30$ for case NR2, where $Y^+ = YU_*/\nu$. By definition, the area under the curve is 1 for either Figure 3 or 4. In Figure 3, $Z_u = (u - U)/\sigma_u$, in which u = local longitudinal velocity, U = local mean longitudinal velocity, and σ_u = standard deviation of the local longitudinal velocity. Similarly, in Figure 4, $Z_v = (v - V)/\sigma_v$, in which v = local vertical velocity, V = local mean vertical velocity, and σ_v = standard deviation of the local vertical velocity. The experimental results as collected by Gupta and

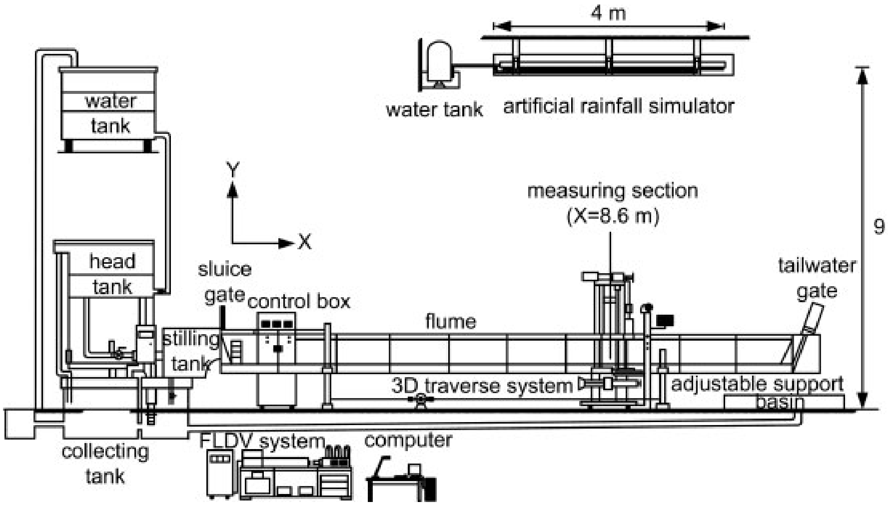

Figure 1. Schematic diagram of the experimental setup and definition of the coordinate system (not to scale)

DOI: 10.1002/hyp

Table I. Summary of data for shallow flows with and without simulated rainfall

Case	S^{a} (%)	I^{b} (mm/h)	d^{c} (mm)	H^{d} (mm)	$\overline{H}^{e}$ (mm)	$\overline{H}/d$	T^{f} (°C)	$Q_1{}^{g}$ (m^3/s)	Q^{h} (m^3/s)	$U_m{}^{i}$ (m/s)	$U_*{}^{j}$ (m/s)	$R_e{}^{k}$
NR1	0·1	0	0	4	—	—	17	0·000118	0·000118	0·059	0·006	218
NR2	1·0	0	0	10	—	—	25	0·002818	0·002818	0·564	0·031	6310
R1	0·1	50·8	3	—	5·76	1·92	17	0·000104	0·000118	0·041	0·007	218
R2	0·1	50·8	4	—	5·87	1·47	17	0·000104	0·000118	0·040	0·008	218
R3	0·1	101·6	3	—	6·08	2·03	17	0·000090	0·000118	0·039	0·008	218
R4	0·1	101·6	4	—	6·14	1·54	17	0·000090	0·000118	0·038	0·008	218
R5	1·0	101·6	4	—	11·37	2·84	24	0·002791	0·002818	0·496	0·033	6159

[a] Channel slope.
[b] Rainfall intensity, 50·8 mm/h = 2 in/h, 101·6 mm/h = 4 in/h.
[c] Raindrop diameter.
[d] Flow depth (without rainfall).
[e] Mean flow depth (with rainfall).
[f] Water temperature.
[g] Flow discharge at the channel entrance.
[h] Flow discharge at the measuring section.
[i] Mean longitudinal velocity in the whole cross section.
[j] Shear velocity = $\sqrt{gRS}$, where g = gravitational acceleration.
[k] Reynolds number = $U_m H / \nu$ (without rainfall), Reynolds number = $U_m \overline{H} / \nu$ (with rainfall), where ν = kinematic viscosity.

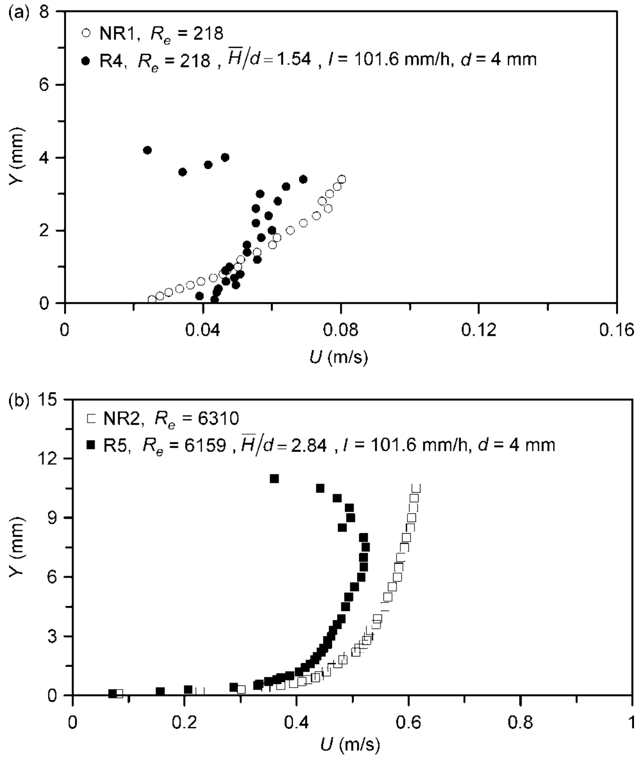

Figure 2. Comparison of mean velocity profiles with and without rainfall: (a) under low Reynolds number, (b) under high Reynolds number

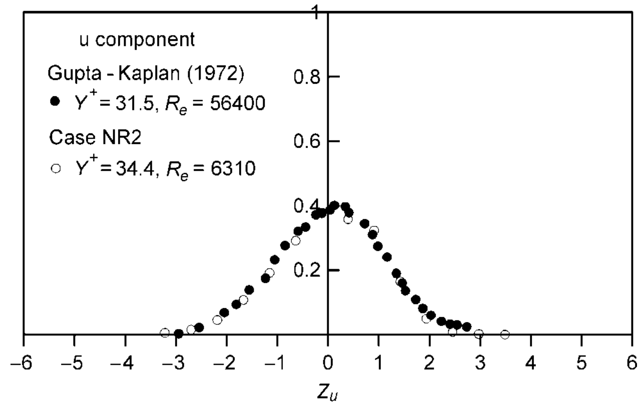

Figure 3. Comparison of normalized probability densities for longitudinal component

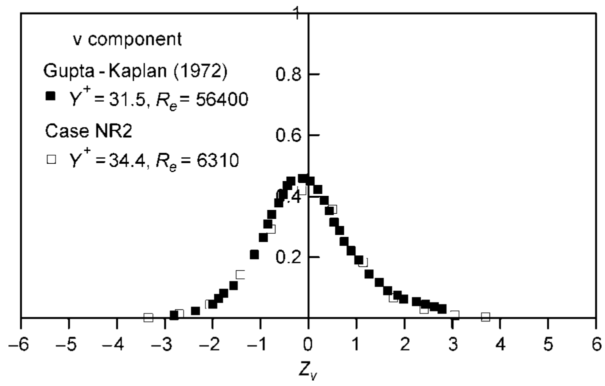

Figure 4. Comparison of normalized probability densities for vertical component

Kaplan (1972) in a wind tunnel using the hot wire probes for $Y^+ \cong 30$ with a high Reynolds number are also plotted in Figures 3 and 4 for comparison. It can be seen that the results from both experiments are reasonably consistent. In addition, the probability densities for both u and v components are fairly close to normal distributions for the wall region ($Y^+ \geq 30$).

Figure 5 shows the normalized probability density function of uv fluctuation at the same position ($Y^+ \cong 30$) for case NR2. Again, Z_{uv} is a standardized form for random variable uv. Both Gupta and Kaplan's data and our experimental results show that the distributions of uv deviate from the Gaussian distribution, and have heavy tails with sharp peak values. Apparently, they are different from the distributions of u and v velocity components.

DOI: 10.1002/hyp

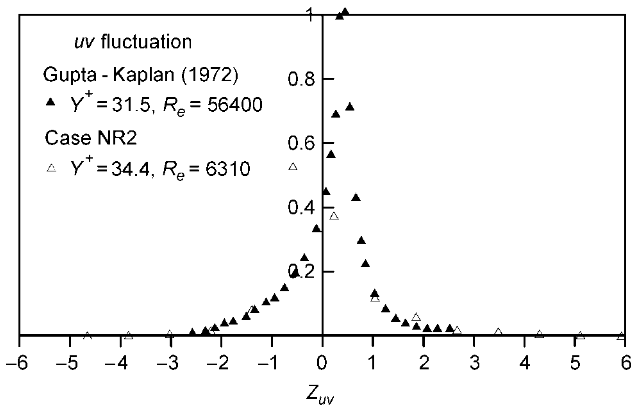

Figure 5. Comparison of normalized probability densities for *uv* fluctuation

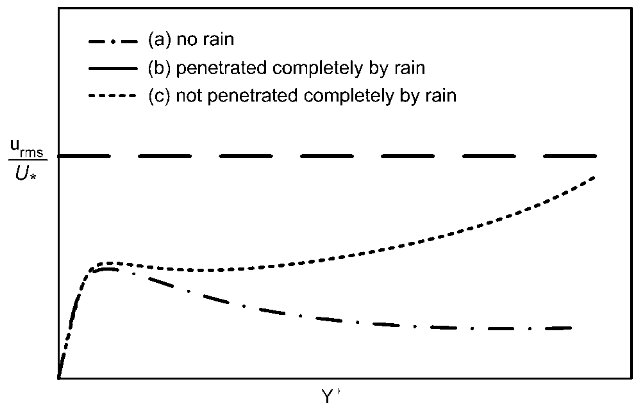

Figure 6. Schematic diagram of the vertical distributions of longitudinal turbulence intensity for shallow flows over smooth bed

Flow penetration by raindrops

Detachment of soil particles is a function of the erosive forces of raindrop impact and flowing water. Macklin and Hobbs (1969) showed that when the surface water depth decreases from 9 mm to 6 mm, the bottom of cavity induced by a raindrop of 2·3 mm diameter becomes increasingly flattened, indicating that the raindrop affected the flow field near the channel bottom.

Lu *et al.* (1998, 2001) proposed a critical penetration depth concept to judge whether the entire flow depth can be penetrated completely by the impacted raindrops. When the flow depth is larger than the critical penetration depth, raindrop impact mainly increase the turbulence properties near the free surface, but will not affect the boundary shear stress. Figure 6 is a schematic diagram showing the vertical distributions of dimensionless longitudinal turbulence intensity u_{rms}/U_*, in which $u_{\mathrm{rms}} = \sqrt{\overline{u'^2}}$; $u' = u - U$ for shallow flows over smooth bed under three different conditions. Curve (a) in Figure 6 is a typical curve for the case without rainfall. When the flow depth is very shallow, the whole depth of the flow is penetrated completely by the raindrops, and u_{rms}/U_* is nearly a constant, as indicated by curve (b) in Figure 6. As the flow depth increases, the flow may not be penetrated completely [curve (c)], and a segment of the distribution of turbulence intensity is overlapped with that without rainfall, i.e. curve (a).

Probability distribution of Reynolds shear stress

With consideration of the random characteristics near the channel boundary under the penetrated condition, all the data within 1 mm (10 points) above the channel bottom are included to calculate the average viscous stress ($\tau_\ell = \mu dU/dY$) and the Reynolds shear stress (τ_t) in the next section. For consistency of comparison, the data within 1 mm above the channel bottom are also used to calculate the values of average viscous stress and the Reynolds shear stress for the cases without rain and under the non-penetrated condition in the next section.

Figures 7a and 7b are comparisons of cumulative probability distributions for the instantaneous Reynolds shear stress ($\tau_t = -\rho u'v'$, where ρ = density of water) with different rainfall intensities and raindrop sizes at $Y = 0{\cdot}1$ mm and $Y = 1$ mm, respectively. One can see that, in general, the tail probability (e.g. $|-\rho u'v'| > 1$ N/m^2) of the instantaneous Reynolds shear stress increases either with an increase of the rainfall intensity (I) or raindrop diameter (d). However, the tail probability is more sensitive to the raindrop diameter as compared to the rainfall intensity. For example, as shown in Table I, the ratio of rainfall intensity of R3 to that of R2 is 2, and the ratio of raindrop diameter of R2 to that of R3 is only 1·33. However, the tail probabilities (e.g. $|-\rho u'v'| > 1$ N/m^2) of R2 is larger than that of R3, as indicated in Figures 7a and 7b.

Kurtosis is a measure of the peakedness of the probability distribution of a real-valued random variable. Higher kurtosis means more of the variance is due to infrequent extreme deviations, as opposed to frequent modestly sized deviations. In contrast to the normal distribution, which has an expected value of zero for the kurtosis, the calculated kurtosis values were 36·4 and 27·6 for R2 and R3 in Figure 7a ($Y = 0{\cdot}1$ mm), and they were 51·1 and 13·0 for R2 and R3 in Figure 7b ($Y = 1$ mm), respectively. The results indicate that the effect of raindrop size on the turbulent shear stress (τ_t) is higher than that of rainfall intensity. Figures 7c and 7d show the probability densities of Reynolds shear stress. One can clearly see that the distributions for R2 and R4 ($d = 4$ mm) have heavy tails, indicating higher probabilities for the occurrence of the extreme shear stress.

In general, for a very shallow flow (e.g. $H = 4$ mm) with intensive raindrop impact (e.g. $I = 101{\cdot}6$ mm/h, $d = 4$ mm in this study), the turbulent boundary shear stress (τ_t) can be either positive or negative. So far as the soil erosion or sediment entrainment is concerned, a negative τ ($\tau = \tau_\ell + \tau_t$) value means that the shear stress is acting in the upstream direction. As long as $|\tau| > \tau_c$, where τ_c is the critical shear stress, the soil erosion or sediment entrainment may occur.

Extreme boundary shear stress

Sediment entrainment or soil particle detachment is a function of both the temporal mean shear stress on the soil surface and the turbulence intensity (or turbulent

DOI: 10.1002/hyp

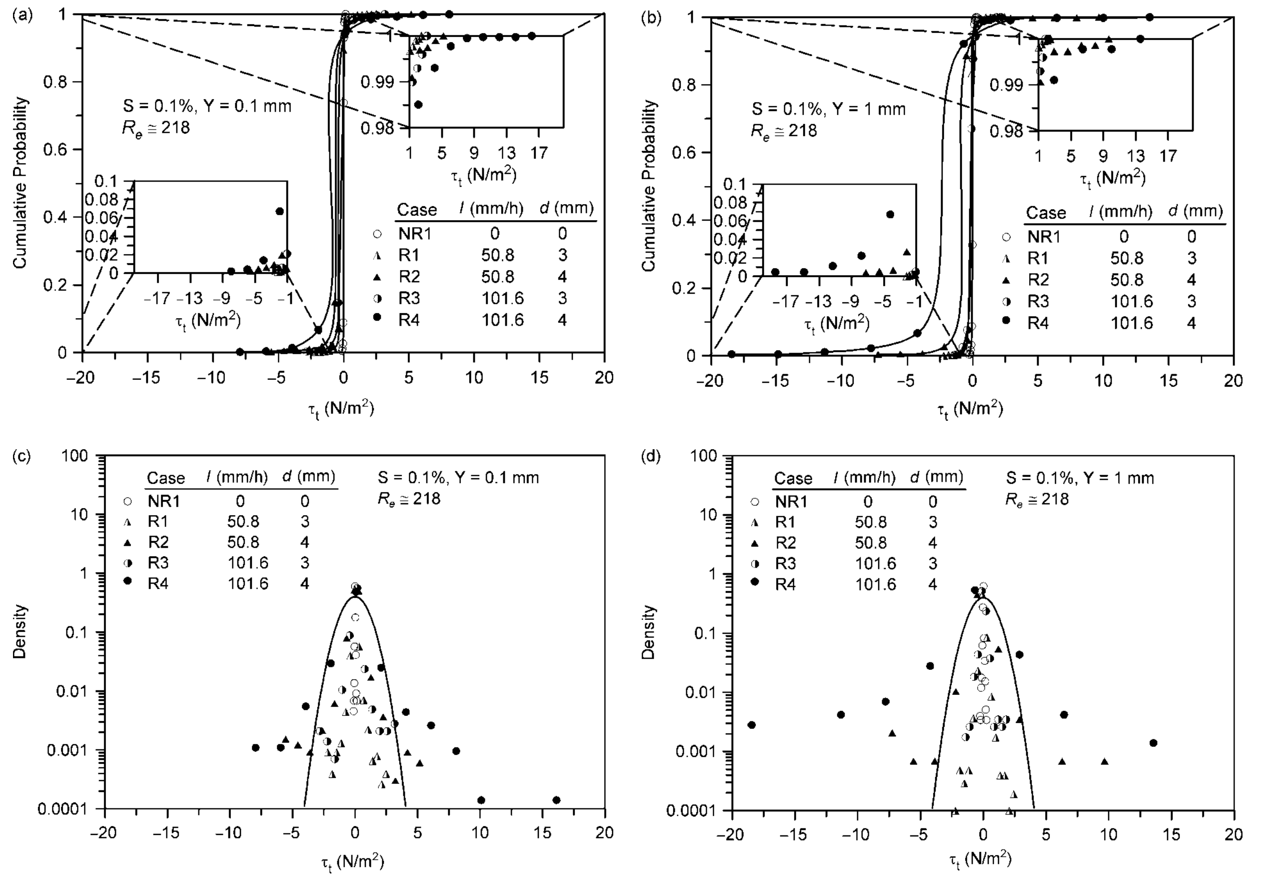

Figure 7. Comparisons of distributions of Reynolds shear stress with different rainfall intensities and raindrop sizes: (a) cumulative distributions, $Y = 0{\cdot}1$ mm; (b) cumulative distributions, $Y = 1$ mm; (c) probability densities, $Y = 0{\cdot}1$ mm; (d) probability densities, $Y = 1$ mm

Table II. Extreme shear stresses near boundary ($Y \leq 1$ mm) under the condition without rain

Case			τ_ℓ (N/m^2)	τ_t (N/m^2)		Empirical 99% confidence limits (N/m^2)		
S (%)	H (mm)	R_e	$\mu\,(dU/dY)$	$\overline{\tau}_t$	$\hat{\sigma}_{\tau_t}$	$\tau_{t,0{\cdot}005}$	$\tau_{t,0{\cdot}995}$	$\tau_{t,0{\cdot}99}/\tau_\ell$ [a]
0.1	4	218	0·036	0·0002	0·042	−0·185	0·153	5·1
0.3	4	522	0·154	0·015	0·225	−1·000	0·785	6·5
0.5	4	956	0·164	0·041	0·366	−1·134	1·301	7·9
1.0	4	1682	0·264	0·228	0·701	−1·790	2·580	9·8
S (%)	H (mm)	R_e	$\mu\,(dU/dY)$	$\overline{\tau}_t$	$\hat{\sigma}_{\tau_t}$	$\tau_{t,0{\cdot}005}$	$\tau_{t,0{\cdot}995}$	$\tau_{t,0{\cdot}99}/\tau_\ell$
0.1	10	1531	0·061	0·039	0·131	−0·419	0·495	8·1
0.3	10	2755	0·227	0·119	0·564	−1·582	2·390	10·5
0.5	10	3955	0·265	0·141	0·744	−2·700	2·619	10·2
1.0	10	6310	0·393	0·488	1·262	−3·832	5·323	13·6

[a] $\tau_{t,0{\cdot}99} = \max(|\tau_{t,0{\cdot}005}|, \tau_{t,0{\cdot}995})$

fluctuation) over it. Based on the qualitative discussions in the previous sections, it is clear that the flow field near the channel bottom is highly disturbed for very shallow flow under heavy rainfall conditions. In the following sections, a quantitative analysis for the raindrop impact on the extreme boundary shear stress is given.

Table II summarizes the calculated boundary shear stress values for cases without rainfall at different slopes and two extreme flow depths ($H = 4$ mm and 10 mm). The viscous shear stress $\tau_\ell = \mu dU/dY$ was calculated from the longitudinal mean velocity profile. The sample mean $\overline{\tau}_t$, sample standard deviation $\hat{\sigma}_{\tau_t}$ of the instantaneous Reynolds shear stress ($\tau_t = -\rho u'v'$) and the empirical 99% confidence limits, including the 0·5% lower limit ($\tau_{t,0{\cdot}005}$) and the 99·5% upper limit ($\tau_{t,0{\cdot}995}$), were calculated from the turbulence measurements. As

Table III. Extreme shear stresses near boundary ($Y \leq 1$ mm) under the condition with rainfall ($I = 101{\cdot}6$ mm/h, $d = 4$ mm)

Case			τ_ℓ (N/m^2)	τ_t (N/m^2)		Empirical 99% confidence limits (N/m^2)		
S (%)	$\overline{H}$ (mm)	R_e	$\mu\,(dU/dY)$	$\overline{\tau}_t$	$\hat{\sigma}_{\tau_t}$	$\tau_{t,0{\cdot}005}$	$\tau_{t,0{\cdot}995}$	$\tau_{t,0{\cdot}99}/\tau_\ell$ [a]
0.1	6·14	218	0·052	0·002	1·437	−8.024	6.148	154·3
0.3	6·13	522	0·154	0·038	1·320	−5.935	5.243	38·5
0.5	6·05	934	0·110	0·131	0·798	−3.398	3.395	30·9
1.0	6·10	1612	0·200	0·221	1·096	−4.283	4.759	23·8
S (%)	$\overline{H}$ (mm)	R_e	$\mu\,(dU/dY)$	$\overline{\tau}_t$	$\hat{\sigma}_{\tau_t}$	$\tau_{t,0{\cdot}005}$	$\tau_{t,0{\cdot}995}$	$\tau_{t,0{\cdot}99}/\tau_\ell$
0.1	11·72	1491	0·130	0·042	0·362	−1·718	1·397	13·2
0.3	11·61	2693	0·190	0·044	0·579	−2·087	2·109	11·1
0.5	11·55	4150	0·220	0·187	0·917	−3·380	3·933	17·9
1.0	11·37	6159	0·355	0·407	1·485	−5·052	6·475	18·2

[a] $\tau_{t,0{\cdot}99} = \max(|\tau_{t,0{\cdot}005}|, \tau_{t,0{\cdot}995})$

the distribution of τ_t is asymmetric, the larger value of $|\tau_{t,0{\cdot}005}|$ and $\tau_{t,0{\cdot}995}$, denoted as $\tau_{t,0{\cdot}99}$, is used to reflect the extreme Reynolds shear stress value, i.e.

$$\tau_{t,0{\cdot}99} = \max(|\tau_{t,0{\cdot}005}|, \tau_{t,0{\cdot}995}) \tag{1}$$

In general, it can be seen that the ratio of $\tau_{t,0{\cdot}99}/\tau_\ell$ increases with an increase of Reynolds number for a given flow depth H under the condition without rain. Table III gives the results for cases under an extreme rainfall condition ($I = 101{\cdot}6$ mm/h, $d = 4$ mm) and with values of R_e close to those in Table II. As shown in Table III, the ratio of $\tau_{t,0{\cdot}99}/\tau_\ell$ increases with a decrease of Reynolds number for cases with Reynolds number less than about 3000. In particular, the extreme Reynolds shear stress can be one to two orders of magnitude larger than the viscous shear stress under the extreme rainfall condition ($I = 101{\cdot}6$ mm/h, $d = 4$ mm) with low Reynolds numbers ($R_e \leq 900$), indicating a significant raindrop impact near the channel boundary.

To illustrate the possible application of the experimental results, Figure 8 shows the relationships between the extreme total shear stress ($\tau = \tau_\ell + \tau_{t,0{\cdot}99}$) and Reynolds number R_e in the region near channel boundary under conditions with and without rain. For the data without rainfall (*hollow circles*), as expected, the extreme total shear stress increases with an increase of Reynolds number due to the increase of flow fluctuations. For the data under extreme rainfall condition (solid circles; $I = 101{\cdot}6$ mm/h, $d = 4$ mm), the extreme total shear stress initially decreases with an increase of Reynolds number up to a R_e value of about 3100, and then it increases with Reynolds number. The results indicate that for R_e less than about 3100 (Zone I, relatively shallower flows), the boundary shear stress is mainly induced by the raindrop impact. In contrast, for R_e greater than about 3100 (Zone II), the raindrop impact is insignificant in the near boundary region, and the turbulent shear stress is dominated by the channel flow turbulence.

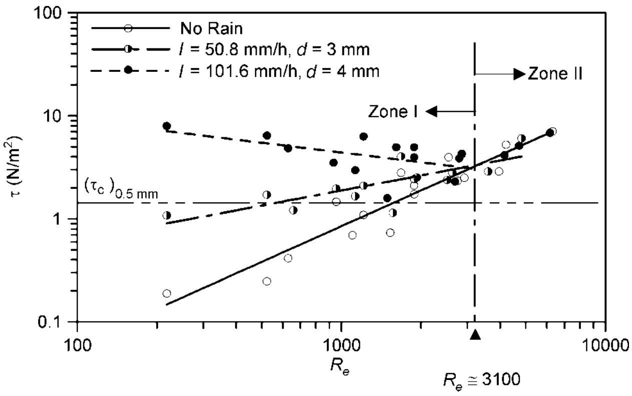

Figure 8. Relationships between the extreme total shear stress ($\tau = \tau_{t,0{\cdot}99} + \tau_\ell$) and Reynolds number in the region near channel boundary under conditions with and without rain. Zone I: raindrop induced turbulence dominated; Zone II: channel flow turbulence dominated

For a non-cohesive particle with 0·5 mm diameter, the permissible unit tractive force (critical shear stress) is about 1·43 N/m^2 (0·03 lb/ft^2; Chow, 1959) for canals with clear water. As shown in Figure 8 (*long dashed line*), most of the extreme total shear stress values under the extreme rainfall condition (*solid circles*) exceed the critical value. However, without rainfall, the Reynolds number has to be greater than about 1600 to cause the particle movement. For comparison, the results for the condition with $I = 50{\cdot}8$ mm/h and $d = 3$ mm (lowest rainfall intensity and smaller raindrop size in this study) are also plotted in Figure 8 (*semi-solid circles*). As expected, the raindrop effect on the boundary shear stress was smaller under this condition as compared to that under the extreme rainfall condition (*solid circles*).

Figure 9 shows the relationships between the dimensionless extreme Reynolds shear stress $\tau_{t,0{\cdot}99}/\tau_\ell$ and Reynolds number for cases without and with extreme rainfall ($I = 101{\cdot}6$ mm/h, $d = 4$ mm). For the case without rainfall, the Reynolds shear stress is mainly induced by the open channel flow, and the ratio $\tau_{t,0{\cdot}99}/\tau_\ell$ increases

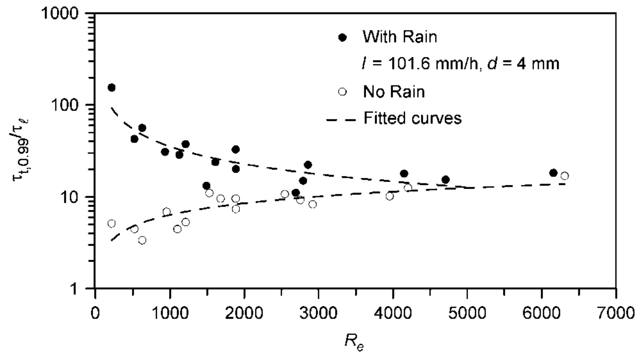

Figure 9. Relationships between the dimensionless extreme Reynolds shear stress ($\tau_{t,0\cdot99}/\tau_\ell$) and Reynolds number

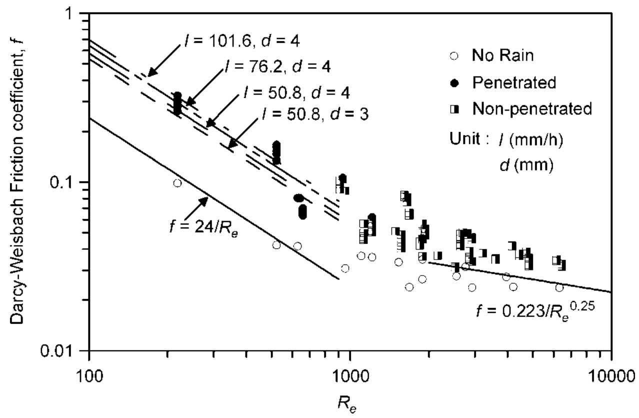

Figure 10. Relationships between Darcy-Weisbach resistance coefficient and Reynolds number with and without raindrop impact

with an increase of Reynolds number R_e. On the contrary, for the case with rainfall, the Reynolds shear stress is mainly induced by the raindrop impact, and the ratio $\tau_{t,0\cdot99}/\tau_\ell$ decreases with an increase of Reynolds number. The two curves converge at a Reynolds number of about 5000. In addition, the extreme Reynolds shear stress $\tau_{t,0\cdot99}$ is about one to two orders of magnitude larger than viscous shear stress τ_ℓ for the case with extreme rainfall condition and low Reynolds number (shallow flow).

Friction coefficient with rainfall

The Darcy-Weisbach resistance coefficient f, for channel flows with and without raindrop impact can be expressed in the following general form:

$$f = \frac{8\tau_0}{\rho U_m^2} \tag{2}$$

where $\tau_0 =$ cross sectional average boundary shear stress $= \gamma RS$; $\gamma =$ specific weight of water; $R =$ hydraulic radius, and $U_{\mathrm{m}} =$ mean longitudinal velocity in the whole cross section. The calculated resistance coefficients against Reynolds number are plotted in Figure 10. The empirical equation $f = 24/R_e$ for laminar flow in rectangular channels (Chow, 1959) and the Blasius equation $f = 0{\cdot}223/R_e^{0\cdot25}$ are also given in Figure 10 for comparison. As shown in Figure 10, in general the present experimental data without rainfall (*hollow circles*) are consistent with these two empirical equations.

Table IV. Comparison of Equations (3) and (4) for shallow flows with simulated rainfall

Formula	Number of tests	Ratio of predicted to measured f value		
		Mean	Standard deviation	r^2
Equation (3)	113	1·059	0·170	0·93
Equation (4)	113	1·018	0·159	0·97

For the data with rainfall, the resistance coefficients are significantly higher than those predicted by the empirical equations mentioned earlier due to the retardation of the rainfall. Shen and Li (1973) derived a regression equation, Equation (3), based on Yoon's (1970) and Li's (1972) data. In contrast to Yoon's (1970) and Li's (1972) experiments where constant raindrop diameters of 3·1 mm and 3·2 mm, respectively were selected, raindrop diameter was a variable in our experiments as shown in Table I. With consideration of the raindrop diameter (d), a new empirical equation, Equation (4), is derived based on Yoon's (1970), Li's (1972) and our experimental data in laminar flow region ($R_e \le 900$). For the convenience of comparison, the units of inch per hour and millimeters are used for I and d in both Equations (3) and (4). The fitted lines based on Equation (4) are also drawn in Figure 10.

$$f = \frac{27{\cdot}162 I^{0\cdot407} + 24}{R_e}, \quad R_e \le 900, \quad r^2 = 0{\cdot}93 \tag{3}$$

$$f = \frac{14{\cdot}531 \times I^{0\cdot503} \times d^{0\cdot342} + 24}{R_e}, \quad R_e \le 900, \quad r^2 = 0{\cdot}97 \tag{4}$$

Table IV summarizes the statistics related to the ratios of predicted to measured f values based on both Equations (3) and (4). One can see that Equation (4) gives a mean value (1·018) closer to 1·0 and a smaller standard deviation (0·159) as compared to Equation (3). Also, Equation (4) provides a higher r^2 value than Equation (3). In other words, with inclusion of raindrop diameter d, Equation (4) gives a slightly better prediction of f values as compared to Equation (3). For natural rainfall, the median raindrop sizes usually increase with rain intensity up to a certain intensity and then tend to remain the same. The empirical relationship between median raindrop size and rain intensity can be developed for each geographic region by field experiments (Lu *et al.*, 2008). Equation (4) can be used for the future development of the physically based soil erosion prediction models.

CONCLUSIONS

This study was undertaken to examine the effect of turbulent fluctuations due to raindrop impact for the shallow flows over smooth bed using a 2-D FLDV. Based on the experimental results, the following conclusions can be drawn:

1. The experimental data indicate that the Reynolds shear stress follows a probability distribution with heavy tails. The tail probability increases with an increase of rainfall intensity or raindrop diameter, and it decreases with an increase of Reynolds number. Furthermore, both the extreme Reynolds shear stress and the extreme tail probability of Reynolds shear stress are more sensitive to the raindrop diameter as compared to the rainfall intensity.
2. In this study, When Reynolds number R_e is less than about 3100, the boundary shear stress is mainly induced by the raindrop impact. In contrast, for R_e greater than about 3100, the raindrop impact is insignificant at the near boundary region, and the turbulent shear stress is dominated by the channel flow turbulence.
3. A modified empirical equation for the calculation of the Darcy-Weisbach friction coefficient f was derived using both the raindrop diameter and rainfall intensity as independent variables. The new equation provided a slightly better prediction of the f values as compared with the original equation developed by Shen and Li (1973).

ACKNOWLEDGEMENTS

This research was funded by the National Science Council of Taiwan, R.O.C. The writers are grateful to Ms. Er-Ling Wu for her experimental assistance.

REFERENCES

Balachandar R, Bhuiyan F. 2007. Higher-order moments of velocity fluctuations in an open-channel flow with large bottom roughness. *Journal of Hydraulic Engineering* **133**(1): 77–87.

Chang FH. 1996. *Turbulence characteristics of rain-impacted free surface flow*. M.S. Thesis, National Chung Hsing University, Taiwan (in Chinese).

Chow VT. 1959. *Open-Channel Hydraulics*. McGraw-Hill Book: New York.

Gupta AK, Kaplan RE. 1972. Statistical characteristics of Reynolds stress in a turbulent boundary layer. *The Physics of Fluids* **15**(6): 981–985.

Hartley DM, Alonso CV. 1991. Numerical study of the maximum boundary shear stress induced by raindrop impact. *Water Resources Research* **27**(8): 1819–1826.

Hartley DM, Julien PY. 1992. Boundary shear stress induced by raindrop impact. *Journal of Hydraulic Research* **30**(3): 341–359.

Kim J, Moin P, Moser R. 1987. Turbulence statistics in fully developed channel flow at low Reynolds number. *Journal of Fluid Mechanics* **177**: 133–166.

Kisisel IIT. 1971. *An experimental investigation of the turbulence characteristics of shallow water flow*. Ph.D. dissertation, Purdue University, W. Lafayette.

Li RM. 1972. *Sheet flow under simulated rainfall*. Ind. M.S. Thesis, Colorado State University, Fort Collins.

Liu JS. 1995. *An experimental study of the effect of rainfall on the flow over a rough bed*. M.S. thesis, National Chung Hsing University, Taiwan (in Chinese).

Lu JY, Chen JY, Chang FH, Lu TF. 1998. Characteristics of shallow rain-impacted flow over smooth bed. *Journal of Hydraulic Engineering* **124**(12): 1242–1252.

Lu JY, Chen JY, Hong JH, Lu TF. 2001. Turbulence intensities of shallow rain-impacted flow over rough bed. *Journal of Hydraulic Engineering* **127**(10): 881–886.

Lu JY, Foster GR, Smith RE. 1987. Numerical simulation of dynamic erosion in a ridge-furrow system. *Transactions of the ASAE* **30**(4): 969–976.

Lu JY, Su CC, Lu TF, Maa MM. 2008. Number and volume raindrop size distributions in Taiwan. *Hydrological Processes* **22**(13): 2148–2158.

Lu SS, Willmarth WW. 1973. Measurements of the structure of the Reynolds stress in a turbulent boundary layer. *Journal of Fluid Mechanics* **60**(3): 481–511.

Macklin WC, Hobbs PV. 1969. Subsurface phenomena and the splashing of drops on shallow liquids.*Science* **166**: 107–108.

Nezu I, Nakagawa H. 1993. *Turbulence in Open-Channel Flows*. A. A. Balkema Publishers: Brookfield.

Raupachu MR. 1981. Conditional statistics of Reynolds stress in rough-wall and smooth-wall turbulent boundary layers. *Journal of Fluid Mechanics* **108**: 363–382.

Shahabian H, Delleur JW. 1976. An experimental investigation of the Rainfall on the turbulence properties of overland flow. Technical report No. 8, Purdue University, W. Lafayette.

Shen HW, Li RM. 1973. Rainfall effect on sheet flow over smooth surface. *Journal of the Hydraulics Division* **99**(HY5): 771–792.

Wenzel HG, Wang RC. 1970. *The Mechanics of a Drop Impact after Striking a Stagnant Water Layer*. Research Report No. 30, University of Illinois Water Res. Center, University of Illinois, Urbana.

Willmarth WW, Lu SS. 1972. Structure of the Reynolds stress near the wall. *Journal of Fluid Mechanics* **55**(1): 65–92.

Wu EL. 2006. *Laboratory experiments for stochastic characteristics of rain-impacted sheet flows over a smooth boundary*. M.S. Thesis, National Chung Hsing University, Taiwan (in Chinese).

Wu FC, Jiang MR. 2007. Numerical investigation of the role of turbulent bursting in sediment entrainment. *Journal of Hydraulic Engineering* **133**(3): 329–334.

Yoon YN.1970. *The effect of rainfall on the mechanics of steady spatially varied sheet flow on a hydraulically smooth boundary*. Ph.D. dissertation, University of Illinois at Urbana-Champaign, Urbana-Champaign.

Yoon YN, Wenzel HG. 1971. Mechanics of sheet flow under simulated rainfall. *Journal of the Hydraulics Division* **97**(HY9): 1367–1386.